Chem. Senses 27: 643–652, 2002

Characterization of cAMP Degradation by Phosphodiesterases in the Accessory Olfactory System

James A. Cherry and Vanee Pho

Department of Psychology and Laboratory of Molecular Neurobiology and Behavior, Boston University, Boston, MA 02215, USA

Correspondence to be sent to: James A. Cherry, Department of Psychology, 64 Cummington Street, Boston University, Boston, MA 02215, USA. e-mail: jcherry@bu.edu

Abstract

To characterize the potential role of cAMP in pheromone transduction, we have examined the occurrence of cyclic nucleotide phosphodiesterases (PDEs) in the mouse vomeronasal organ (VNO). We show that the cAMP-specific isoforms PDE4A and PDE4D are found preferentially in the apical and basal layers, respectively, of the VNO neuroepithelium and in the rostral (PDE4A) and caudal (PDE4D) portions of the accessory olfactory bulb glomerular layer. Assays for cAMP hydrolysis showed that PDE activity in VNO homogenates was about half that measured in the cerebral cortex and olfactory epithelium, and the proportion of total activity inhibited by rolipram, a PDE4-specific inhibitor, was ~40%. Activity in the VNO was enhanced 60% by Ca^{2+} and calmodulin (CaM), implicating the presence of Ca^{2+}/CaM-dependent PDE1. Zaprinast, which is known to inhibit PDE1C isoforms, completely suppressed Ca^{2+}/CaM-stimulated activity and, together, zaprinast and rolipram inhibited cAMP hydrolysis by ~70%. Our results suggest that PDE1 and PDE4 isoforms are the primary source of cAMP degradation in the VNO.

Introduction

Responses to pheromones are mediated in part by an accessory olfactory pathway that begins in receptor neurons of the vomeronasal organ (VNO). For rodents in particular, these neurons appear to be anatomically and neurochemically divided into apical and basal layers, from which axons project to non-overlapping rostral and caudal glomeruli in the accessory olfactory bulb—the AOB (Halpern *et al.*, 1998). From the AOB, projections are then made to subcortical targets in the amygdala and hypothalamus. In contrast to the neuroanatomical organization, far less is known about how pheromones are processed in the mammalian VNO.

In the main olfactory system, generation of the cyclic nucleotide cAMP is an essential component of the pathway by which odors lead to the depolarization of olfactory sensory neurons (Pace *et al.*, 1985; Sklar *et al.*, 1986). However, whether cAMP plays a similar (or any) role in the transduction of pheromones in the mammalian VNO is unclear. Adenylyl cyclases ACII (Berghard and Buck, 1996) and ACVI (Rossler *et al.*, 2000), as well as the cAMP hydrolyzing enzyme PDE4A (Lau and Cherry, 2000) are present in the mammalian VNO, but studies in which cAMP levels have been measured in the VNO after exposing animals or isolated membranes to pheromones have been conflicting (Zhou and Moss, 1997; Sasaki *et al.*, 1999; Rossler *et al.*, 2000). Although a cyclic-nucleotide-gated channel subunit is expressed in VNO neurons, cyclic-nucleotide-gated channel conductance has not been detected (Liman and Corey, 1996). Rather, most current evidence points to a primary role of an inositol 1,4,5-triphosphate (IP_3) pathway in pheromonal signaling in mammals (Inamura *et al.*, 1997; Wekesa and Anholt, 1997; Liman *et al.*, 1999).

To understand better the role of cAMP in the accessory olfactory system, it will be important to identify the primary regulators of cAMP levels in the VNO. In particular, there has been little attention focused on the enzymes responsible for the breakdown of cAMP—the cyclic nucleotide phosphodiesterases (PDEs). These proteins consist of 11 distinct families grouped according to biochemical and pharmacological properties, although only eight families are known to hydrolyze cAMP (Francis *et al.*, 2001). For example, the Type I PDEs (PDE1) consist of enzymes that can hydrolyze both cAMP and cGMP and are activated by Ca^{2+} and calmodulin (CaM). Meanwhile, PDE4s are characterized by high affinity and specificity for cAMP as a substrate, as well as sensitivity to inhibition by the PDE4-specific inhibitor rolipram. In olfactory sensory neurons, the predominant PDE activity is generated by Ca^{2+}-dependent PDE1 subtype(s) and the Ca^{2+}-independent PDE4s (Borisy *et al.*, 1992). In addition, an olfactory-specific member of the cGMP-stimulated PDE2 family has been localized to a

© Oxford University Press 2002. All rights reserved.

restricted group of sensory neurons in the olfactory epithelium (Juilfs *et al.*, 1997).

Previously, we showed that the PDE4 isoform, PDE4A, is selectively found in apical VNO neurons and their targets in the rostral AOB glomeruli (Lau and Cherry, 2000). We now report that a second PDE4 isoform, PDE4D, is present in the accessory olfactory system. Using isoform-specific antibodies, we show that PDE4D occurs primarily in basal VNO neurons and caudal AOB glomeruli. In addition, we have used an assay for cAMP hydrolysis to measure PDE activity in the VNO and found that PDE4 enzymes make up ~40% of overall cAMP hydrolysis under basal conditions. Elevated PDE activity measured in the presence of Ca^{2+} and CaM suggests that PDE1 enzymes also contribute significantly to overall cAMP hydrolysis in the VNO. Our results indicate that two differentially localized PDE4 isoforms and one or more PDE1 enzymes are the principal regulators of cAMP breakdown in the VNO.

Materials and methods

Materials

Radiochemicals 2,8-[^{3}H]cAMP and 2,8-[^{3}H]adenosine were obtained from NEN (Boston, MA). Rolipram, milrinone, 3-isobutyl-1-methylxanthine (IBMX) and zaprinast were obtained from RBI (Natick, MA). Diethyl-(2-hydroxypropyl)aminoethyl (QAE) Sephadex A-25, protease inhibitors [phenylmethylsulfonyl fluoride (PMSF), aprotinin, pepstatin A, antipain, chymostatin and leupeptin], snake venom (*Crotalus atrox*) and all reagents and chemicals not otherwise identified were from Sigma (St Louis, MO).

Tissue preparation

Adult, Swiss Webster mice of both sexes were used in all experiments. Tissues were prepared for immunohistochemistry as described previously (Cherry and Davis, 1999). For PDE assays and immunoblot analysis, animals were killed by decapitation and tissues, including brain, VNO, olfactory epithelium, heart, liver and kidney, were rapidly dissected, frozen on dry ice and placed at –80°C. Just prior to use, tissues were homogenized in ice-cold buffer (20 mM Tris, pH 7.5, 0.2 mM $MgCl_2$, 0.25 M sucrose, 1% Triton X-100, 0.5 mM PMSF, 3 μM pepstatin, 3 μM leupeptin, 2 μg/ml aprotinin, 1 μg/ml antipain, 2 μg/ml chymostatin). Protein concentrations of homogenates were determined by Bradford analysis (Bio-Rad, Hercules, CA). Except where indicated, separately prepared homogenates consisted of tissues provided by at least three different animals. The use of animals followed National Institutes of Health guidelines and was approved by the Boston University Animal Care and Use Committee.

Olfactory bulbectomy

Eight adult mice were anesthetized with xylazine and ketamine and a small incision was made in the scalp overlying the olfactory bulbs. The skin was retracted and a small hole was drilled through the skull to expose the olfactory bulbs. Suction was applied through a glass pipette and the olfactory bulbs were removed by aspiration. Gel-foam was packed into the cavity and the skin was sutured shut. Mice were allowed to recover for several hours under heat lamps before returning to the colony rooms.

Immunohistochemistry

VNOs from four animals were cryosectioned coronally at 20 μm onto poly-L-lysine-coated glass slides and dried overnight. Frozen sections of the AOB were cut sagittally at 30 μm and placed free-floating into phosphate-buffered saline (PBS). Sections were processed for immunohistochemistry with affinity-purified, rabbit polyclonal anti-PDE4A and anti-PDE4D antibodies (Cherry and Davis, 1999) and a 1:200 (VNO) or 1:500 (AOB) dilution of secondary antibody (biotinylated goat anti-rabbit immunoglobulin; Vector Laboratory, Burlingame, CA). Control sections in which the primary antibodies were omitted were also included. Tissue was then reacted with Vector Elite ABC reagent and product was visualized with 1 mg/ml 3′,3′-diaminobenzidine and 0.03% H_2O_2. Photomicrographs of selected regions were taken with a Nikon DXM 1200 digital camera mounted on an Olympus BX-60 microscope. Final images were cropped and assembled in Adobe Photoshop, v. 6.0 (Adobe Systems Inc., San Jose, CA). Brightness and contrast were adjusted for each photomicrograph to achieve uniform image quality.

Immunoblotting

Aliquots of tissue homogenates containing 10–20 μg of protein were separated by sodium dodecyl sulfate polyacrylamide gel electrophoresis (SDS–PAGE) and transferred to Immobilon-P membranes (Millipore Corporation, Bedford, MA). Membranes were then processed for immunoblotting with anti-PDE4A, anti-PDE4B, or anti-PDE4D antibodies. The secondary antibody was a 1:2500 dilution of horseradish-peroxidase-conjugated goat anti-rabbit immunoglobulin (Bio-Rad) and immunoreactive proteins were visualized using chemiluminescence reagent (NEN, Boston, MA). Signals were recorded on BioMax Imaging film (Eastman Kodak, Rochester, NY) and scanned into Adobe Photoshop. To examine the effects of olfactory bulbectomy (BX) on PDE4 levels, band intensities were determined for sham-treated and BX animals on adjacent blots processed at the same time on the same piece of film. Optical densities were obtained using MultiAnalyst (BioRad) and signal density differences between groups were compared statistically using Student's *t*-tests.

PDE assay

Activity of cyclic nucleotide PDEs was determined using a modification of the Thompson and Appleman (Thompson and Appleman, 1971) two-step procedure (Bauer and

Schwabe, 1980; Cherry *et al.*, 2001). Briefly, tubes were prepared consisting of 20 µl of diluted tissue homogenate in 40 mM Tris–HCl, pH 8.0, 5 mM $MgCl_2$, 40 000 c.p.m. [^{3}H]cAMP and cold cAMP. Final sample volumes were 200 µl and, except for assays in which substrate concentration was specifically varied, all reactions were conducted at 1 µM cAMP. Tubes were incubated at 30°C for 10 min, then transferred briefly into an ethanol/dry ice bath before placing in boiling water for 45 s. Snake venom (25 µl of 2 mg/ml) was added for an additional 10 min incubation before applying the reaction mixture to equilibrated chromatography columns (BioRad) containing QAE Sephadex A-25. Cyclic AMP PDE activity was computed from the eluates and expressed as nmol cAMP hydrolyzed/mg protein/min.

Stock solutions of 625 µg/ml CaM and 1 M $CaCl_2$ were prepared in 40 mM Tris–HCl, pH 8.0. Rolipram, milrinone, zaprinast and IBMX were prepared as 10 mM solutions in ethanol and diluted as necessary before adding to tissue tubes in 2 µl aliquots. When these reagents were used, 2 µl of ethanol were also added to control tubes with no apparent effect on PDE activity.

Samples were run in duplicate or triplicate and averaged. For the determination of cAMP hydrolysis in different tissues, two separate preparations of homogenates derived from at least three animals were assayed at least twice each on different days. Assay results were averaged for each homogenate, and final data presented as the mean (±SEM) of the averages for the two homogenates (n = 2). For the olfactory BX experiment, samples were obtained from individual animals and differences in PDE activity between control and BX animals were examined statistically with Student's t-tests. Statistical tests comparing percentages were performed on data after arcsin transformation.

For the experiment comparing the effects of various inhibitors and Ca^{2+} environment on cAMP hydrolysis in the VNO, six VNO homogenates containing VNOs from at least three animals were prepared. Each homogenate was assayed in duplicate under each drug and Ca^{2+} condition, and the mean PDE activities in different groups were compared statistically with Student's t-tests for paired samples. For the rolipram + zaprinast + IBMX condition, only two homogenates were used.

Results

Immunolocalization of PDE4 isoforms

Labeling within the VNO neuroepithelium after staining with anti-PDE4A antibody was robust and confined primarily to sensory neurons in the apical layer, as shown in Figure 1A (Lau and Cherry, 2000). However, a different pattern of immunoreactivity was observed with the PDE4D-specific antibody (Figure 1B). Overall, anti-PDE4D labeling was weaker in comparison to anti-PDE4A, but nevertheless appeared limited to sensory neurons and not supporting cells. Basal VNO neurons seemed more darkly stained by the PDE4D antibody than apical cells, but labeling intensity between these populations was not as distinct as that observed with anti-PDE4A antibody. At higher magnification (Figure 1C), labeling was seen in dendrites and perikarya of PDE4D-stained neurons, but there was no staining in the neuronal microvilli that line the lumen of the VNO, where chemosignal transduction is believed to initiate. Although staining in the neuroepithelium was relatively weak, the most significant labeling appeared to be in clumps of cells along the basal layer. Axon bundles (not seen here) were also labeled by both antibodies.

In the rodent, projections from apical and basal VNO neurons terminate in rostral and caudal glomeruli of the AOB, respectively (Jia and Halpern, 1996; Belluscio *et al.*, 1999; Rodriguez *et al.*, 1999). Consistent with this anatomical arrangement, brain sections exposed to anti-PDE4A antibody were stained in the rostral half of AOB glomerular layer, as shown in Figure 1D (Lau and Cherry, 2000). Conversely, we found that PDE4D immunoreactivity in the AOB was restricted to the caudal half of the glomerular layer (Figure 1E). The relative difference between rostral/caudal PDE4D staining intensity in the AOB was considerably greater than the staining differences observed between apical and basal VNO neurons. A control VNO section in which the primary antibody was omitted during processing was not stained (Figure 1F).

Immunoblots prepared from tissue homogenates of the VNO, olfactory epithelium and cerebral cortex were next examined using antibodies that specifically recognize either PDE4A, PDE4B, or PDE4D subtypes (Cherry and Davis, 1999). For these blots, equal amounts (20 µg) of protein were loaded per lane to show the relative levels of PDE4 enzyme in each of the tissues. Single proteins of 105 and 100 kDa were revealed in the VNO by the anti-PDE4A and anti-PDE4D antibodies, respectively, whereas no signal was observed with anti-PDE4B (Figure 2). All three antibodies recognized PDE4 proteins in the cortex and PDE4A was most abundant in olfactory epithelium. In contrast, only trace PDE4B and PDE4D immunoreactivity was observed in olfactory epithelium, suggesting that PDE4A is the predominant PDE4 enzyme in this tissue. Control blots in which the primary antibody was omitted were completely blank (data not shown).

Finally, to verify that PDE4 expression in the VNO occurs primarily in neurons, olfactory bulbs were removed bilaterally. This procedure results in the selective degeneration of most VNO neurons in response to the removal of their target sites in the AOB, whereas nonsensory components of the VNO remain largely unaffected (Barber and Raisman, 1978). Examination of immunoblots of VNOs from BX and sham-treated animals indicated that mean PDE4A expression was significantly reduced after BX [$t(6) = 4.44$, $P < 0.005$] and that mean PDE4D levels were also reduced in such animals compared to controls (Figure 3). For PDE4D,

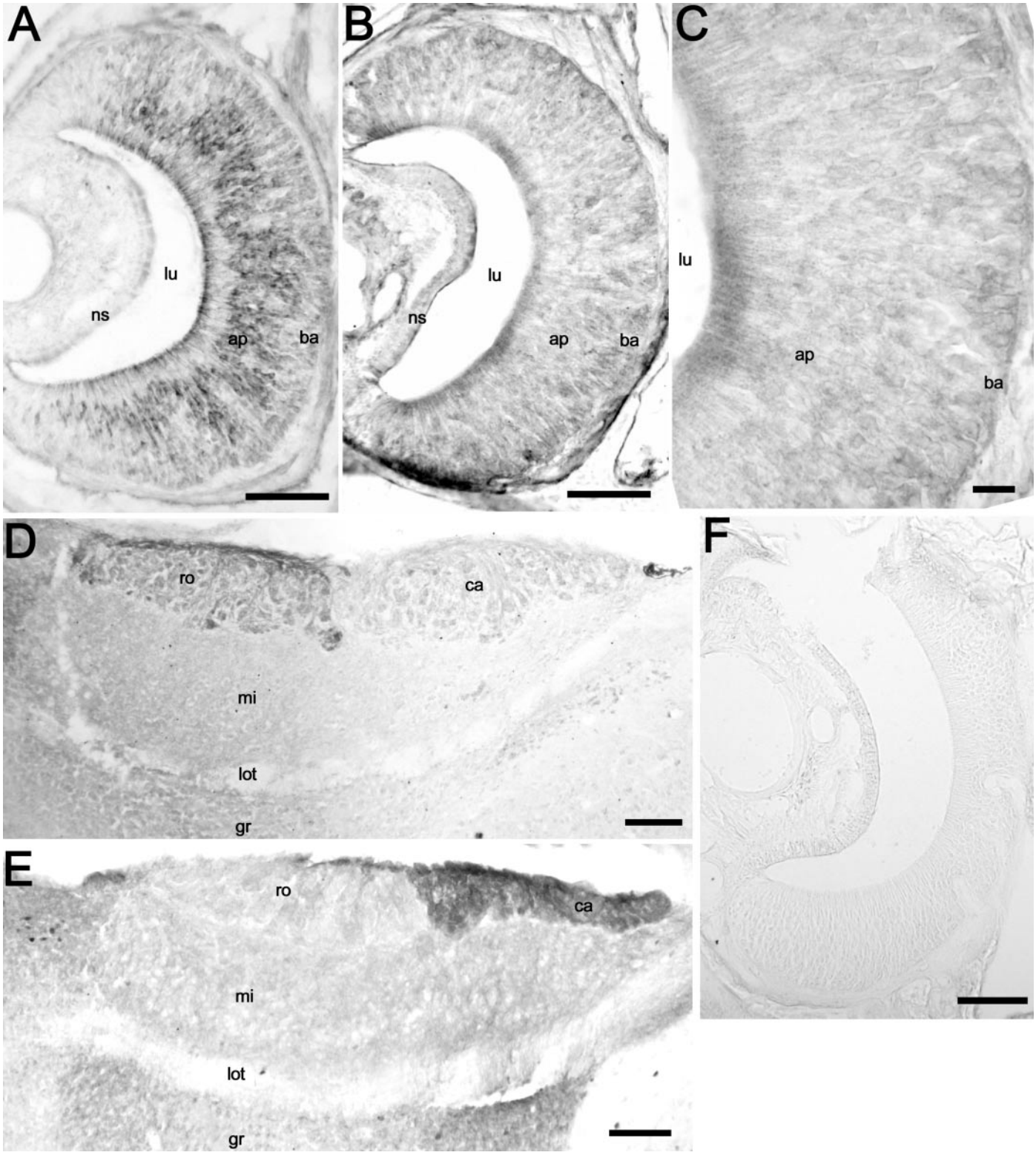

Figure 1 Antibodies against PDE4D and PDE4A label different zones of the accessory olfactory pathway. In **(A)**, incubation of VNO sections with anti-PDE4A antibody strongly labels apical sensory neurons (ap). In **(B)**, light labeling of VNO sensory neurons is seen in the neuroepithelium with anti-PDE4D antibody, with neurons in the basal layer (ba) appearing to be more immunoreactive. At higher magnification **(C)**, PDE4D-immunoreactive signal in basal cells is relatively weak, and no signal is observed in the sensory microvilli that line the lumen (lu). In **(D)**, anti-PDE4A antibody stains glomeruli in the rostral (ro) half of the AOB, whereas anti-PDE4D antibody labels caudal (ca) glomeruli **(E)**. A control section in which the primary antibody was omitted does not stain **(F)**. Other abbreviations: gr, granule cell layer; lot, lateral olfactory tract; mi, mitral cell layer; ns, nonsensory epithelium. Scale bars: 20 μm (C); 100 μm for all other panels.

this reduction was of borderline significance [$t(6) = 2.21$, $P < 0.07$]. Thus, PDE4A and PDE4D levels after BX were on average only 10 and 40% of control values, respectively, providing additional evidence that both PDE4 subtypes occur in sensory neurons.

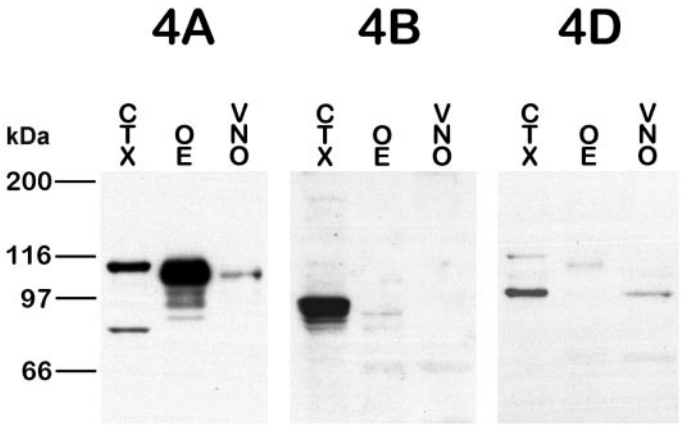

Figure 2 Immunoblots of mouse cerebral cortex (CTX), olfactory epithelium (OE) and VNO are shown following incubation with affinity purified, isoform-specific anti-PDE4 antibodies. In the left panel, immunoreactive bands are seen in all tissues with anti-PDE4A antibody (4A). An isolated, 105 kDa band is present in the VNO lane that migrates with the dominant protein observed in the olfactory epithelium. In the center panel, anti-PDE4B antibody (4B) recognizes a major protein of 90 kDa in the CTX, but has no immunoreactivity for proteins in the olfactory epithelium and VNO. In the right panel, anti-PDE4D (4D) antibody reveals a single 100 kDa species in the VNO that migrates with the dominant protein seen in the CTX. A faint signal of ~110 kDa is also seen with this antibody in the olfactory epithelium.

cAMP PDE activity

In addition to the PDE4 enzymes, members of at least seven other PDE families can hydrolyze cAMP. Therefore, the total level of PDE activity measured in our assay reflects the combined contribution of all cAMP-hydrolyzing enzymes present in the tissue. We first examined and compared the overall level of PDE activity in the VNO with other tissues. As shown in Figure 4, total PDE activity was greatest in cerebral cortex, olfactory bulb and olfactory epithelium, lowest in heart and liver, and intermediate in the VNO and kidney.

To determine the proportion of activity in the VNO that was attributable to different PDEs, the effects of various PDE inhibitors (all used at 100 μM) were examined both in the presence and absence of 100 μM Ca^{2+} and 4 μg/ml CaM (Figure 5). In the absence of inhibitors, addition of Ca^{2+}/CaM increased cAMP hydrolysis significantly from 0.12 ± 0.014 to 0.19 ± 1.7 nmol/mg protein/min, an increase of 61% [$t(5) = 9.9$, $P < 0.001$], suggesting that a Ca^{2+}-dependent PDE is present in the VNO. The PDE4-specific inhibitor rolipram reduced cAMP hydrolysis by 40% in the absence of Ca^{2+}/CaM and 27% in the presence of Ca^{2+}/CaM. Although both reductions are significant [$t(4) = 6.6$, $P < 0.005$; $t(4) = 8.4$, $P < 0.001$, respectively], these results indicate that

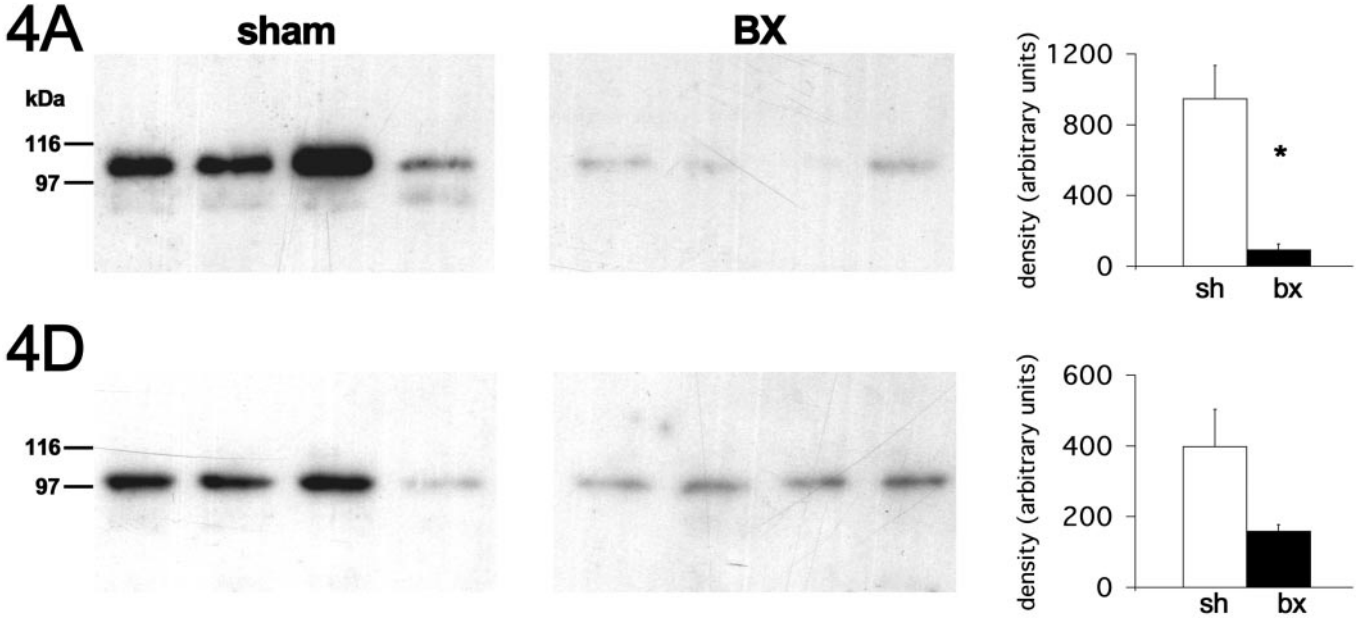

Figure 3 Expression of PDE4 isoforms in the VNO decreases after bilateral olfactory bulbectomy (BX). Vomeronasal organs obtained from four sham and four BX mice 7 days after surgery were homogenized, loaded in adjacent lanes (20 μg protein/lane) and separated by SDS–PAGE. The resulting blots were incubated with antibodies against PDE4A (top panel) and PDE4D (bottom panel). Blots were exposed on the same piece of film following chemiluminescence processing and exposure time was adjusted to enable faint bands to be revealed. Immunoreactive bands were quantified by densitometry and means (±SEM) for each group are shown in the graphs on the right. BX significantly reduced the level of PDE4A (*$P < 0.005$) in comparison to sham-operated controls, and the decrease in PDE4D levels after BX was of borderline significance ($P < 0.07$).

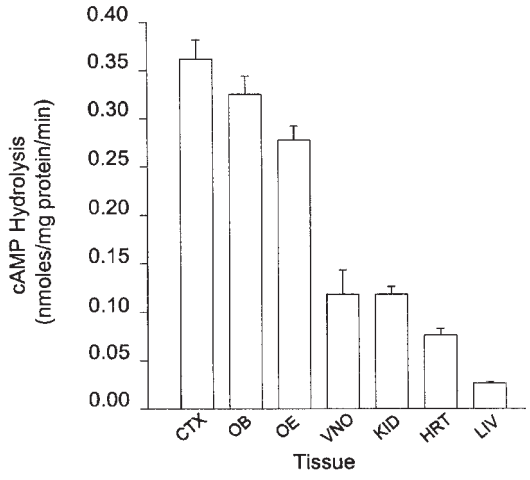

Figure 4 The level of PDE activity measured in homogenates of different mouse tissues is shown using 1 μM cAMP as a substrate. Highest rates of cAMP hydrolysis were measured in brain (cerebral cortex, CTX; olfactory bulb, OB) and olfactory epithelium (OE) and lowest levels were observed in liver (LIV). The level of PDE activity in the VNO was about half that measured in the olfactory epithelium. For each tissue, two different homogenates were assayed in duplicate at least twice each. These measures were averaged for each homogenate, and data are plotted as the mean (±SEM) of these averages (n = 2 for each tissue). Other abbreviations: HRT, heart; KID, kidney.

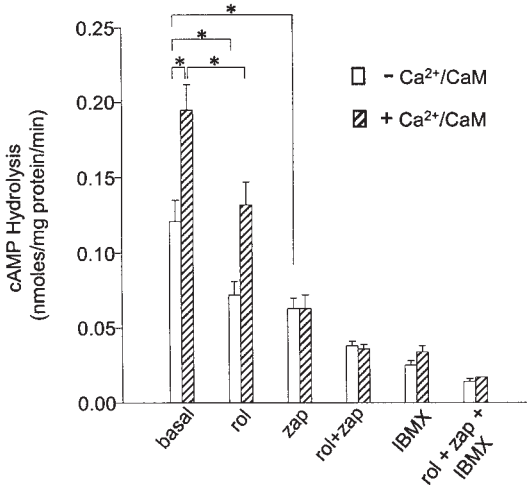

Figure 5 The effects of inhibitors on the mean (±SEM) level of PDE activity in VNO homogenates is shown in the absence (open bars) or presence (striped bars) of 100 μM Ca^{2+} and 4 μg/ml CaM; n = 5 independent measurements from different homogenates (each in duplicate) for all bars except rol + zap + IBMX, where n = 2. Asterisks over bracketed groups indicate statistically significant ($P < 0.05$) differences based on Student's t-tests for paired samples. Abbreviations: rol, rolipram; zap, zaprinast.

PDE4s account for less than half of the total VNO PDE activity, even under basal conditions.

Zaprinast, which is generally considered a PDE5/6 inhibitor (Beavo, 1995), has also more recently been shown to inhibit several isoforms of the PDE1 family (Loughney *et al.*, 1996). While completely suppressing the increase in PDE activity observed with Ca^{2+}/CaM [zap – Ca^{2+} versus zap + Ca^{2+}, $t(4) = 1.7$, $P = 0.16$], zaprinast inhibited cAMP hydrolysis by 48% versus basal controls in the absence of Ca^{2+}/CaM [$t(4) = 7.4$, $P = 0.002$; Figure 5]. We have shown elsewhere, however, that zaprinast can also significantly reduce PDE4 activity: cAMP hydrolysis by a PDE4A subtype (mouse PDE4A1) transiently transfected in HEK293 cells was 45% inhibited by 100 μM zaprinast versus 95% inhibition by 100 μM rolipram [unpublished observations and Cherry *et al.* (Cherry *et al.*, 2001)]. This suggests that zaprinast in the present study inhibited both PDE1 and PDE4 activity in VNO homogenates, a conclusion supported by the observation that zaprinast and rolipram inhibition was not additive (68% inhibition by zaprinast + rolipram compared to 40 and 48% by rolipram or zaprinast alone, respectively).

The generic PDE inhibitor IBMX alone reduced PDE activity by 85% and at a slightly higher level (92%) when added to samples in combination with rolipram and zaprinast (Figure 5). This indicates that only a small proportion of cAMP PDE activity in the VNO can be accounted for by IBMX-insensitive PDEs, such as PDE8 (Fisher *et al.*, 1998). As for other IBMX-sensitive PDEs, there is evidence from the rat that isoforms of the cGMP-stimulated PDE2 and cGMP-inhibited PDE3 families may be present in the olfactory epithelium (Borisy *et al.*, 1992). However, in data not shown, we failed to find any effect of adding either 1 μm cGMP or 100 μM of the PDE3 inhibitor milrinone on cAMP PDE activity in homogenates from the mouse VNO.

Finally, we examined PDE activity in VNOs from animals given bilateral BX. Olfactory BX significantly reduced overall mean PDE activity by about half in comparison to control animals that received sham operations [Figure 6; $t(19) = 3.8$, $P < 0.002$]. Interestingly, the mean proportion of rolipram-inhibitable PDE activity from VNOs of BX animals was significantly greater than for controls [Figure 6; 47 ± 5.3% versus 32 ± 4.8%, $t(19) = 2.12$, $P < 0.05$]. This indicates that despite the loss of neurons and the reduction in the levels of PDE4A and PDE4D that occurs following BX (Figure 3), a relatively higher proportion of remaining total cAMP PDE activity is due to PDE4 enzymes in comparison to controls.

Discussion

Activation of cyclic nucleotides by G-protein-coupled receptors is a feature of transduction in virtually all sensory systems. In olfaction, taste, vision and mechanosensation, generation of either cAMP or cGMP occurs in direct response to a sensory stimulus, implicating PDEs as important regulators of cyclic nucleotide levels. Although the role of cAMP in the VNO remains to be determined, our data indicate that multiple PDE enzymes are present in this tissue. Moreover, the segregated distribution of two PDE4 isoforms that we have described in the accessory olfactory

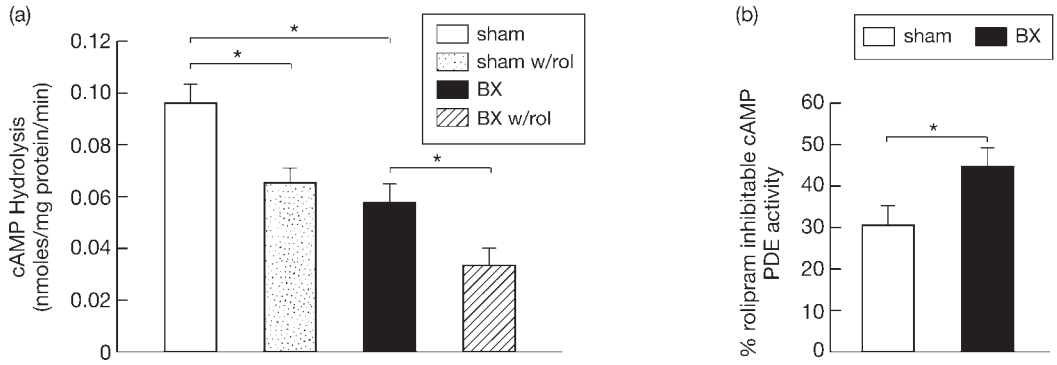

Figure 6 Bilateral olfactory bulbectomy (BX) significantly reduced cAMP PDE activity in VNO homogenates. In the left graph, mean (±SEM) rates of cAMP hydrolysis in VNO homogenates are shown with and without rolipram from animals that received sham ($n = 12$) or bilateral BX ($n = 9$) 7 days previously. BX significantly decreased the overall rate of cAMP hydrolysis relative to sham-operated controls ($P < 0.002$) and rolipram reduced PDE activity in both sham and BX groups ($P < 0.05$ for both comparisons). However, a higher proportion of rolipram-inhibitable activity was present in VNO homogenates after BX versus controls (right graph, $P < 0.05$).

system suggests that the regulation of cAMP may differ in apical and basal VNO neurons and their projections.

Our study provides anatomical evidence that PDE4s occur in different subpopulations of VNO neurons. As shown previously (Lau and Cherry, 2000), PDE4A was found predominantly in apical VNO neurons and in rostral AOB glomeruli. In contrast, several observations support the contention that PDE4D is expressed in VNO neurons but more so in basal than apical neurons. Despite relatively poor resolution, PDE4D appeared by immunocytochemical methods to occur mostly in basal neurons. In addition, immunoblot analysis indicated that 7 days after BX, PDE4D levels were reduced in accord with the dramatic loss of neurons that occurs after lesion. Finally, we showed that caudal AOB glomeruli, which receive projections exclusively from basal VNO neurons, were more heavily stained by PDE4D antibody than the adjacent rostral glomeruli.

There are several explanations for why two closely related PDE4 isoforms would be preferentially expressed in different sets of VNO neurons. In general, proteins encoded by PDE4A and PDE4D genes display similar biochemical characteristics: all isoforms examined to date are low K_m enzymes inhibited by micromolar concentrations of rolipram. However, comparison of individual proteins expressed from alternative splice forms of each gene has revealed differences in rolipram sensitivity, subcellular distribution and interaction with other proteins. For example, the RD1 splice variant of PDE4A is exclusively membrane associated, whereas PDE4A5, which differs only in the N-terminal domain, is distributed in both the cytosolic and particulate fractions of both brain and transfected COS cell extracts (McPhee *et al.*, 1995). Similarly distinct patterns of subcellular distribution have been found for other PDE4 isoforms found in the brain (Lobban *et al.*, 1994; Bolger *et al.*, 1997). In addition, differences in binding of PDE4 subtypes to other proteins have been described. The PKC-binding scaffold protein RACK1 selectively binds to the N-terminal region of the PDE4D5 isoform (Yarwood *et al.*, 1999) and only the PDE4D4 and PDE4A5 subtypes have been shown to interact with SH3 domains found in various kinases (Beard *et al.*, 1999). Functionally, such interactions could alter the catalytic activity of the enzyme, or, alternatively, increase local concentrations of PDE4s by recruitment to protein complexes involved in specific signaling pathways (Pawson and Scott, 1997; Houslay *et al.*, 1998). Thus, the regulation of cAMP by PDE4s within a cell may depend not only on the kinetic properties of individual subtypes, but also upon their subcellular distribution and the presence of specific interacting proteins.

Our results indicate that only single PDE4A and PDE4D proteins occur in the VNO. On immunoblots labeled with PDE4D antibody, a 100 kDa protein was identified from VNO homogenates that likely represents the product of the splice form PDE4D3. This enyzme is the smallest of three 'long' PDE4D isoforms that have been characterized (Bolger *et al.*, 1997). Little, however, is known about the 105 kDa PDE4A protein that was found in both the VNO and olfactory epithelium. In brain, this protein is found only in the olfactory bulbs (Cherry and Davis, 1995), although it is not yet known whether it is expressed intrinsically in olfactory bulb cells or is localized only in axons from chemosensory cells. This unique isoform may therefore represent a protein encoded by a novel PDE4A splice form that is specific to chemosensory tissue. A third PDE4 examined in this study, PDE4B, was not localized in the VNO and the other member of this class, PDE4C, is virtually absent from the rodent nervous system (Bolger *et al.*, 1994; Engels *et al.*, 1995).

The presence of PDE4 proteins in the VNO was confirmed by examination of cAMP hydrolysis in VNO homogenates. Overall, the level of cAMP PDE activity we measured in the mouse VNO was about half that measured in the olfactory epithelium. Thus, despite the differences in signal transduction components that exist between the

olfactory epithelium and VNO (Berghard *et al.*, 1996), cAMP PDE activity was represented in both tissues. This included a significant proportion of both rolipram-inhibited as well as Ca^{2+}/CaM-activated PDE activity (Borisy *et al.*, 1992). A prospective candidate to account for the Ca^{2+}-activated PDE activity in the VNO is PDE1C2. This protein is a PDE1 isoform found in olfactory sensory neurons and is particularly abundant in olfactory cilia (Yan *et al.*, 1995). The presence of PDE1C would also be consistent with the finding that PDE activity in the VNO was markedly decreased in the presence of zaprinast, which effectively inhibits PDE1C subtypes (Loughney *et al.*, 1996; Han *et al.*, 1999).

Our data suggest that most cAMP hydrolysis in the VNO is attributable to PDE1 and PDE4 isoforms, but that other PDEs may be present at lower levels. Overall, IBMX inhibited cAMP hydrolysis by 85%, leaving only 15% of activity that could be due to IBMX-insensitive isoforms. Of the two families of IBMX-insensitive PDEs so far documented, only PDE8 enzymes use cAMP as a substrate. However, PDE8 isoforms are also insensitive to rolipram and zaprinast (Fisher *et al.*, 1998; Hayashi *et al.*, 1998) and in VNO homogenates, only 8% of activity remained in samples containing IBMX + zaprinast + rolipram versus controls. Thus, cAMP hydrolysis in the VNO due to PDE8 activity is probably minor.

In contrast, 68% of cAMP hydrolysis was inhibited in the VNO by zaprinast + rolipram, which implicates PDE1 and PDE4 isoforms as the primary regulators of cAMP breakdown in the VNO. The contributions of all other IBMX-sensitive PDEs in the VNO are represented in the additional 17% of cAMP PDE activity that was inhibited by IBMX but not by rolipram and/or zaprinast. Enzymes fitting these criteria have been described in the PDE2, PDE7 and PDE10 families (Beavo, 1995; Soderling *et al.*, 1999). Further studies will be needed to determine if particular isoforms from any of these families contribute to cAMP hydrolysis in the VNO.

After BX, reductions in levels of both PDE4A and PDE4D were observed. However, despite these decreases in PDE4 protein levels, the proportion of rolipram-inhibitable PDE activity that remained after BX actually increased. In rats, levels of olfactory marker protein (OMP) increase in neurons remaining in the olfactory epithelium following BX (Carr *et al.*, 1998) and we have observed similar increases in PDE4A immunoreactivity in olfactory sensory neurons of the mouse (Cherry, unpublished observations). Although it is not known why either OMP or PDE4A would be up-regulated in olfactory neurons that survive removal of target sites in the olfactory bulb, a BX-induced increase in the relative proportion of rolipram-inhibitable (PDE4) PDE activity seems to occur in VNO neurons as well.

There is now strong evidence that PDE4 enzymes are present in sensory neurons of both the main and accessory olfactory systems (Borisy *et al.*, 1992; Cherry and Davis, 1995; Lau and Cherry, 2000). What remains to be determined is the specific functional role of each enzyme. In addition to its localization in apical neurons of the VNO, PDE4A is also found in mature receptor cells of the olfactory epithelium. Lack of PDE4A in the olfactory cilia of these neurons, however, suggests that rather than participating directly in the early steps of the transduction process, its function may be somewhere downstream. Similarly, both PDE4A and PDE4D seem to be absent from microvilli, the receptor-bearing structures of the VNO. A possible role of dendritic and somatic PDEs has been suggested by studies on deciliated olfactory receptor cells of the salamander. In dissociated cells, application of adrenaline increased both the threshold for firing and the number of spikes generated in response to strong stimuli, responses which were dependent on phosphorylation by cAMP-dependent protein kinase (Kawai *et al.*, 1999). Thus, dendrosomatically localized PDEs could affect sensory perception by increasing the contrast between chemosignals of different concentrations.

The role of different second messenger systems in chemosignal transduction by the vertebrate VNO is currently unresolved. Studies in a variety of species have provided evidence that IP_3 may be involved in the VNO response to chemosignals (Luo *et al.*, 1994; Inamura *et al.*, 1997; Wekesa and Anholt, 1997; Krieger *et al.*, 1999; Sasaki *et al.*, 1999). In addition, a novel member of the transient receptor potential family of ion channels (TRP2) has been cloned and found to be exclusively localized in VNO microvilli (Liman *et al.*, 1999). Evidence that TRP channels can be activated by diacylglycerol (Hofmann *et al.*, 1999) provides a possible mechanism by which IP_3 induction might lead to opening of TRP2 in the VNO after pheromonal stimulation.

However, the role that cAMP plays in VNO chemosignal transduction is less clear, particularly for mammalian species. There are reports that cAMP levels are unchanged in the male hamster VNO following stimulation by female chemosignals (Kroner *et al.*, 1996), but in the mouse, exposure to urine-derived compounds decreases levels of cAMP generated in the VNO (Zhou and Moss, 1997). A recent study in the rat has examined the time course of both IP_3 and cAMP production during application of urinary components to preparations of microvilli from VNO neurons (Rossler *et al.*, 2000). Whereas these stimuli induced a rapid IP_3 signal, they also generated a delayed and prolonged decrease in cAMP. This indicates that both IP_3- and cAMP-mediated pathways are activated by exposure to pheromones, but with unique temporal—and perhaps spatial—characteristics. Thus, a scenario can be envisioned whereby IP_3-dependent events could be induced by pheromones initially in the sensory microvilli and, later, modulatory influences on transduction by cyclic nucleotides located in other neuronal compartments could occur. More studies will be needed to test this possibility.

Acknowledgements

We appreciate the assistance of Yanny Lau with immunohistochemistry and thank Drs M.J. Baum and J.-W. Lin for reviewing earlier versions of the manuscript. This study was supported by NIH grant DC03019.

References

Barber, P.C. and **Raisman, G.** (1978) *Replacement of receptor neurones after section of the vomeronasal nerves in the adult mouse.* Brain Res., 147, 297–313.

Bauer, A.C. and **Schwabe, U.** (1980) *An improved assay of cyclic 3′, 5′-nucleotide phosphodiesterases with QAE-Sephadex columns*. Naunyn-Schmiedeberg's Arch. Pharmacol., 311, 193–198.

Beard, M.B., O'Connell, J.C., Bolger, G.B. and **Houslay, M.D.** (1999) *The unique N-terminal domain of the cAMP phosphodiesterase PDE4D4 allows for interaction with specific SH3 domains*. FEBS Lett., 460, 173–177.

Beavo, J.A. (1995) *Cyclic nucleotide phosphodiesterases: functional implications of multiple isoforms.* Physiol. Rev., 75, 725–748.

Belluscio, L., Koentges, G., Axel, R. and **Dulac, C.** (1999) *A map of pheromone receptor activation in the mammalian brain*. Cell, 97, 209–220.

Berghard, A. and **Buck, L.B.** (1996) *Sensory transduction in vomeronasal neurons: Evidence for Gαo, Gαi, and adenylyl cyclase II as major components of a pheromone signaling cascade*. J. Neurosci., 16, 909–918.

Berghard, A., Buck, L.B. and **Liman, E.R.** (1996) *Evidence for distinct signaling mechanisms in two mammalian olfactory sense organs*. Proc. Natl Acad. Sci. USA, 93, 2365–2369.

Bolger, G.B., Rodgers, L. and **Riggs, M.** (1994) *Differential CNS expression of alternative mRNA isoforms of the mammalian genes encoding cAMP-specific phosphodiesterases*. Gene, 149, 237–244.

Bolger, G.B., Erdogan, S., Jones, R.E., Loughney, K., Scotland, G., Hoffman, R., Wilkinson, I., Farrell, C. and **Houslay, M.D.** (1997), *Characterization of five different proteins produced by alternatively spliced mRNAs from the human cAMP-specific phosphodiesterase PDE4D gene*. Biochem. J., 328, 539–548.

Borisy, F., Ronnett, G., Cunningham, A., Juilfs, D., Beavo, J. and **Synder, S.** (1992) *Calcium/calmodulin activated phosphodiesterase expressed in olfactory receptor neurons*. J. Neurosci., 12, 915–923.

Carr, V.M., Walters, E., Margolis, F.L. and **Farbman, A.I.** (1998) *An enhanced olfactory marker protein immunoreactivity in individual olfactory receptor neurons following olfactory bulbectomy may be related to increased neurogenesis.* J. Neurobiol., 34, 377–390.

Cherry, J.A. and **Davis, R.L.** (1995) *A mouse homolog of dunce, a gene important for learning and memory in* Drosophila*, is preferentially expressed in olfactory receptor neurons*. J. Neurobiol., 28, 102–113.

Cherry, J.A. and **Davis, R.L.** (1999) *Cyclic AMP phosphodiesterases are localized in regions of the mouse brain associated with reinforcement, movement and affect*. J. Comp. Neurol., 407, 287–301.

Cherry, J.A., Thompson, B.A. and **Pho, V.** (2001) *Diazepam and rolipram differentially inhibit cyclic AMP-specific phosphodiesterases PDE4A1 and PDE4B3 in the mouse.* Biochim. Biophys. Acta, 1518, 27–35.

Engels, P., Abdel'Al, S., Hulley, P. and **Lübbert, H.** (1995) *Brain distribution of four rat homologues of the* Drosophila *dunce cAMP phosphodiesterase*. J. Neurosci. Res., 41, 169–178.

Fisher, D.A., Smith, J.F, Pillar, J.S., St Denis, S.H. and **Cheng, J.B.** (1998) *Isolation and characterization of PDE8A, a novel human cAMP-specific phosphodiesterase.* Biochem. Biophys. Res. Commun., 246, 570–577.

Francis, S.H., Turko, I.V. and **Corbin, J.D.** (2001) *Cyclic nucleotide phosphodiesterases: relating structure and function.* Prog. Nucleic Acid Res. Mol. Biol., 65, 1–52.

Halpern, M., Jia, C. and **Shapiro, L.S.** (1998) *Segregated pathways in the vomeronasal system.* Microsc. Res. Tech., 41, 519–529.

Han, P., Werber, J., Surana, M., Fleischer, N. and **Michaeli, T.** (1999) *The calcium/calmodulin-dependent phosphodiesterase PDE1C down-regulates glucose-induced insulin secretion.* J. Biol. Chem., 274, 22337–22344.

Hayashi, M., Matsushima, K., Ohashi, H., Tsunoda, H., Murase, S., Kawarada, Y. and **Tanaka, T.** (1998) *Molecular cloning and characterization of human PDE8B, a novel thyroid-specific isozyme of 3′,5′-cyclic nucleotide phosphodiesterase.* Biochem. Biophys. Res. Commun., 250, 751–756.

Hofmann, T., Obukhov, A.G., Schaefer, M., Harteneck, C., Gudermann, T. and **Schultz, G.** (1999) *Direct activation of human TRPC6 and TRPC3 channels by diaclyglycerol*. Nature, 397, 259–263.

Houslay, M.D., Sullivan, M. and **Bolger, G.B.** (1998) *The multienzyme PDE4 cyclic adenosine monophosphate-specific phosphodiesterase family: intracelluar targeting, regulation, and selective inhibition by compounds exerting anti-inflammatory and anti-depressant actions*. Adv. Pharmacol., 44, 225–342.

Inamura, K., Kashiwayanagi, M. and **Kurihara, K.** (1997) *Blockage of urinary responses by inhibitors for IP3-mediated pathway in rat vomeronasal sensory neurons*. Neurosci. Lett., 233, 129–32.

Jia, C. and **Halpern, M.** (1996) *Subclasses of vomeronasal receptor neurons: Differential expression of G proteins ($Gi_{\alpha 2}$ and Go_{α}) and segregated projections to the accessory olfactory bulb*. Brain Res., 719, 117–128.

Juilfs, D.M., Fulle, H.-J., Zhao, A.Z., Houslay, M.D., Garbers, D.L. and **Beavo, J.A.** (1997) *A subset of olfactory neurons that selectively express cGMP-stimulated phosphodiesterase (PDE2) and guanylyl cyclase-D define a unique olfactory signal transduction pathway*. Proc. Natl Acad. Sci. USA, 94, 3388–3395.

Kawai, F., Kurahashi, T. and **Kaneko, A.** (1999) *Adrenaline enhances odorant contrast by modulating signal encoding in olfactory receptor cells.* Nat. Neurosci., 2, 133–138.

Krieger, J., Schmitt, A., Lobel, D., Gudermann, T., Schultz, G., Breer, H. and **Boekhoff, I.** (1999) *Selective activation of G protein subtypes in the vomeronasal organ upon stimulation with urine-derived compounds.* J. Biol. Chem., 274, 4655–4662.

Kroner, C., Breer, H., Singer, A. and **O'Connell, R.J.** (1996) *Pheromone-induced second messenger signaling in the hamster vomeronasal organ*. Neuroreport, 7, 2989–2992.

Lau, Y.E. and **Cherry, J.A.** (2000) *Distribution of PDE4A and Go_{α} immunoreactivity in the accessory olfactory system of the mouse*. Neuroreport, 11, 27–32.

Liman, E.R. and **Corey, D.P.** (1996) *Electrophysiological characterization of chemosensory neurons from the mouse vomeronasal organ*. J. Neurosci., 16, 4625–4637.

Liman, E.R., Corey, D.P. and **Dulac, C.** (1999) *TRP2: a candidate transduction channel for mammalian pheromone sensory signaling*. Proc. Natl Acad. Sci. USA, 96, 5791–5796.

Lobban, M., Shakur, Y., Beattie, J. and **Houslay, M.D.** (1994) *Identification of two splice variant forms of type-IV_B cyclic AMP*

phosphodiesterase, DPD (rPDE-IV$_{B1}$) and PDE-4 (rPDE-IV$_{B2}$) in brain: selective localization in membrane and cytosolic compartments and differential expression in various brain regions. Biochem. J., 304, 399–406.

Loughney, K., Martins, T.J., Harris, E.A.S., Sadhu, K., Hicks, J.B., Sonnenburg, W.K., Beavo, J.A. and **Ferguson, K.** (1996) *Isolation and characterization of cDNAs corresponding to two human calcium, calmodulin-regulated, 3′,5′-cyclic nucleotide phosphodiesterases*. J. Biol. Chem., 271, 796–806.

Luo, Y., Lu, S., Chen, P., Wang, D. and **Halpern, M.** (1994) *Identification of chemoattractant receptors and G-proteins in the vomeronasal system of garter snakes*. J. Biol. Chem., 269, 16867–16877.

McPhee, I., Pooley, L., Lobban, M., Bolger, G. and **Houslay, M.D.** (1995) *Identification, characterization and regional distribution in brain of RPDE-6 (RNPDE4A5), a novel splice variant of the PDE4A cyclic AMP phosphodiesterase*. Biochem. J., 310, 965–974.

Pace, U., Hanski, E., Salomon, Y. and **Lancet, D.** (1985) *Odorant-sensitive adenylate cyclase may mediate olfactory reception*. Nature, 316, 255–258.

Pawson, T. and **Scott, J.D.** (1997) *Signaling through scaffold, anchoring, and adaptor proteins*. Science, 278, 2075–2080.

Rodriguez, I., Feinstein, P. and **Mombaerts, P.** (1999) *Variable patterns of axonal projections of sensory neurons in the mouse vomeronasal system.* Cell, 97, 199–208.

Rossler, P., Kroner, C., Krieger, J., Lobel, D., Breer, H. and **Boekhoff, I.** (2000) *Cyclic adenosine monophosphate signaling in the rat vomeronasal organ: role of an adenylyl cyclase type VI*. Chem. Senses, 25, 313–322.

Sasaki, K., Okamoto, K., Inamura, K., Tokumitsu, Y. and **Kashiwayanagi, M.** (1999) *Inositol-1,4,5-triphosphate accumulation induced by urinary pheromones in female rat vomeronasal epithelium.* Brain Res., 823, 161–168.

Sklar, P.B., Anholt, R.R. and **Snyder, S.H.** (1986) *The odorant-sensitive adenylate cyclase of olfactory receptor cells. Differential stimulation by distinct classes of odorants.* J. Biol. Chem., 261, 15538–15543.

Soderling, S.H., Bayuga, S.J. and **Beavo, J.A.** (1999) *Isolation and characterization of a dual-substrate phosphodiesterase gene family: PDE10A.* Proc. Natl Acad. Sci. USA, 96, 7071–7076.

Thompson, W.J. and **Appleman, M.M.** (1971) *Multiple cyclic nucleotide phosphodiesterase activities from rat brain.* Biochemistry, 10, 311–316.

Wekesa, K.S. and **Anholt, R.R.H.** (1997) *Pheromone regulated production of inositol-(1,4,5)-trisphosphate in the mammalian vomeronasal organ*. Endocrinology, 138, 3497–3504.

Yan, C., Zhao, A.Z., Bentley, J.K., Loughney, K., Ferguson, K. and **Beavo, J.A.** (1995) *Molecular cloning and characterization of a calmodulin-dependent phosphodiesterase enriched in olfactory sensory neurons*. Proc. Natl Acad. Sci. USA, 92, 9677–9681.

Yarwood, S.J., Steele, M.R., Scotland, G., Houslay, M.D. and **Bolger, G.B.** (1999) *The RACK1 signaling scaffold protein selectively interacts with the cAMP-specific phosphodiesterase PDE4D5 isoform*. J. Biol. Chem., 274, 14909–14917.

Zhou, A. and **Moss, R.L.** (1997) *Effect of urine-derived compounds on cAMP accumulation in mouse vomeronasal cells*. Neuroreport, 8, 2173–2177.

Accepted June 13, 2002